Effect of n-type barrier doping on steady and dynamic performance of InGaN light-emitting diodes*

CHEN Gui-chu (陈贵楚)[1,2]** **and FAN Guang-han** (范广涵)[2]

1. Department of Electronic Information, Zhao Qing University, Zhaoqing 526061, China

2. Institute of Optoelectronic Material and Technology, South China Normal University,Guangzhou 510631, China

(Received 10 March 2014)

The steady and dynamic properties are comparatively investigated for the n-doped and non-doped InGaN LEDs. The simulated results show that the n-doped LED exhibits the superior luminescence and modulation performance, which is mainly attributed to the higher carrier radiative rate of n-doped LED. The results can explain the reported experimental results perfectly.

Document code: A **Article ID:** 1673-1905(2014)04-0250-3

DOI 10.1007/s11801-014-4033-7

The visible III-nitride light-emitting diodes (LEDs) have received much attention due to their wide applications in full-color display, liquid crystal display back-lighting, mobile platforms and illumination[1-3]. Another potential application of GaN-based LEDs is for visible light communications (VLCs) in both free space and fiber-based embodiments. Plastic optical fiber (POF) is widely used as a transmission medium for in-building data networks. McKendry and his team[4,5] have reported micro-pixellated GaN-based LED arrays with 3-dB bandwidth up to 300 MHz per pixel in a VLC system. Shi et al[6,7] have obtained about 100 MHz modulation bandwidth of green InGaN/GaN LED in a POF communication system.

In this work, a set of rate equations of the InGaN LED are built based on a circuit simulator. The simulation results accord with the experimental results measured by Shi[7], and reveal that the enhanced carrier radiative rate results in the superior performance of the n-type noped LED.

Two LEDs named samples A and B in Ref.[6] are considered here, in which each quantum well in the active region consists of 13.5 nm GaN barrier and 2.5 nm InGaN well. The structures of both samples are the same except the n-type barrier doping in sample A. Thus the dynamics of carriers and photons is described in terms of the following two nonlinear differential equations mentioned below[8], which form the basis of the circuit model:

$$\frac{\mathrm{d}n}{\mathrm{d}t}=\frac{I}{qV_{\mathrm{act}}}-(An+Bn^2+Cn^3), \tag{1}$$

$$\frac{\mathrm{d}s}{\mathrm{d}t}=Bn^2-\frac{s}{\tau_{\mathrm{p}}}, \tag{2}$$

where n denotes the electron density (cm^{-3}) in the active region, I is the injected current, q is the electronic charge, V_{act} is the volume of the active region, s is the photon density, τ_{p} is the lifetime of photon, and A, B and C are the non-radiative coefficient, radiative coefficient and Auger coefficient, respectively. V_{act} is equal to $NA_{\mathrm{c}}(L_{\mathrm{w}}+L_{\mathrm{b}})$, where N is the number of quantum wells, A_{c} is the area of the cross section, and L_{w} and L_{b} are the widths of the well and barrier.

In order to derive the equivalent circuit representation from Eqs.(1) and (2), the standard circuit elements are brought to transform the rate equations into the specific type which is suitable for the formation of the circuit model. The non-radiative coefficient A is considered to be equal to $1/\tau_{\mathrm{nr}}$, and τ_{nr} is denoted as the non-radiative lifetime of carriers, so the non-radiative recombination current I_{n} is equal to $qV_{\mathrm{act}}n/\tau_{\mathrm{nr}}$, while the radiative recombination current and Auger recombination current are expressed as bI_{n}^2 and cI_{n}^3, respectively, where $b=B/(AqV_{\mathrm{act}})^2$ and $c=C/(AqV_{\mathrm{act}})^3$. The carrier population in the active region is also defined as

$$n=n_0\exp(\frac{qV_{\mathrm{j}}}{\eta kT}), \tag{3}$$

where n_0 is the equilibrium carrier density in the active region, V_{j} is the voltage across the active region, η is the corresponding diode ideality factor, typically set equal to 2, and T is the absolute temperature. The differential term $qV_{\mathrm{act}}\mathrm{d}n/\mathrm{d}t$ of Eq.(1) can be denoted as a product of C_{j} and $\mathrm{d}V_{\mathrm{j}}/\mathrm{d}t$, with C_{j} expressed as

$$C_{\mathrm{j}}=\frac{q^2V_{\mathrm{act}}n_0}{\eta kT}\exp(\frac{qV_{\mathrm{j}}}{\eta kT}), \tag{4}$$

* This work has been supported by the National Natural Science Foundation of China (No.61176043).

** E-mail:gchenbox@126.com

where C_j is the capacitance representing the charge storage effect in the active region. However, the type of Eq.(2) is not effective to form corresponding circuit model and some improvements must be adopted to satisfy this requirement. The optical output power P_{out} [9] can be represented by a nodal voltage, namely,

$$V_{out}(V) = P_{out}(W) = \frac{\eta_0 A_c hc^2}{6\lambda_s} s = \alpha s \,, \tag{5}$$

where η_0 is the extracted light efficiency of LED, λ_s is the peak wavelength, h is the Planck's constant, and c is the velocity of light. With these modifications, Eqs.(1) and (2) are transformed into the following types:

$$I = I_n + bI_n^2 + cI_n^3 + C_j \frac{dV_j}{dt} \,, \tag{6}$$

$$bI_n^2 = \frac{V_{out}}{R_s} + C_s \frac{dV_{out}}{dt} \,, \tag{7}$$

where $R_s=\alpha\tau_p$, $C_s=1/\alpha$. The circuit model based on Eqs.(6) and (7) is formed in Fig.1.

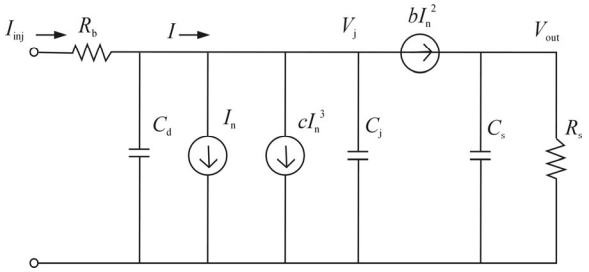

Fig.1 The equivalent circuit model of LED derived from rate equations

I_{inj} is the total injected current of LED with the parasitic elements R_b and C_d, where R_b is considered to be equal to the differential resistance derived from the Shi's measured *V-I* curve[6], and C_d is a diffusion capacitance, which is added into the circuit model for generalizing Eq.(6). $C_d=C_0(1-V_j/V_d)^{-1/2}$, where C_0 is the zero-bias diffusion capacitance, V_j is equal to that in Eq.(4), and V_d is the diode built-in potential.

Although the circuit model of LED in Fig.1 is a strict large-signal variety, it allows a small-signal analysis over the desired frequency range, by simply adding a small-signal current source connected with the dc bias source in parallel. The bias currents required to yield specified values of steady-state optical output power would be obtained from prior dc simulations. The values of the parameters used in our simulation are listed in Tab.1[6,10,11].

Fig.2 shows the light-current characteristics of both samples. The *P-I* curves are derived from the dc SPICE simulation of our circuit model. We can see that the simulated curves accord with the experimental data basically. All the *P-I* curves fall when the injected current is greater than a special value, which is due to the Auger radiation dominates the recombination process in both samples. The superior *P-I* performance of sample A to sample B can be attributed to the higher radiative coefficient B, lower non-radiative coefficient A and Auger coefficient C in sample A with n-type doping, compared with non-doped sample B. The lower A means the less defects in the layer epitaxy of LED, which explains that the epitaxy of MOW with n-doping can achieve excellent interface quality[6].

Tab.1 Model parameters used in the simulation

Symbol	Description	Sample A	Sample B
A	Non-radiative coefficient	2.5×10^{9} s^{-1}	3.3×10^{9} s^{-1}
B	Radiative coefficient	3.6×10^{-11} s^{-1}	2.2×10^{-11} s^{-1}
C	Auger coefficient	8.4×10^{-35} s^{-1}	1.2×10^{-34} s^{-1}
τ_p	Lifetime of photon	2.5 ps	Unchanged
λ_S	Peak wavelength	496 nm	518 nm
η_0	Extracted light efficiency	0.1	Unchanged
A_c	Area of cross section	14 000 μm^2	Unchanged
C_0	Zero-bias diffusion capacity	85 pF	Unchanged
V_d	Built-in potential	4.5 V	4.2 V

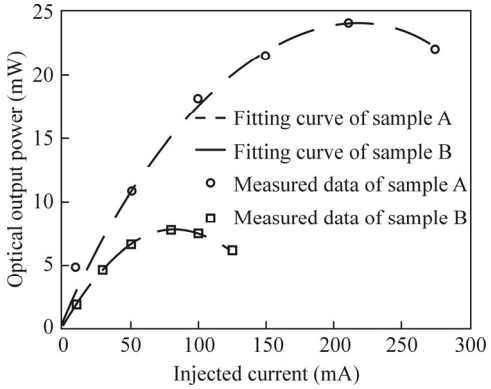

Fig.2 Output optical power versus the injected current for samples A and B

Fig.3 shows the frequency responses of samples A and B at 50 mA bias current. The simulated modulation responses derived from the ac simulation of Spice model are close to the measured data for both samples. Sample A exhibits wider 3-dB bandwidth than sample B, which can be explained by two facts as follows. Firstly, the n-doped sample A has smaller body resistance R_b and diffusion capacitance C_d than non-doped sample B, which will decrease the R_bC_d time constant of LED. Secondly, the spontaneous recombination time influenced by the n-type doping is another factor to affect the modulation speed[6], which is verified by the fact that the higher radiative coefficient B of Sample A is adopted in the simulation. But our calculated limited bandwidths $R_b(C_d+C_j)$ of both LEDs' circuits are much wider than the obtained 3-dB bandwidths in Fig.3, which clearly shows that the radiative rate is a more influential factor

than *RC* constant to limit the bandwidth. Especially speaking, the experimental results of Shi[6] also support our theoretical conclusion mentioned above.

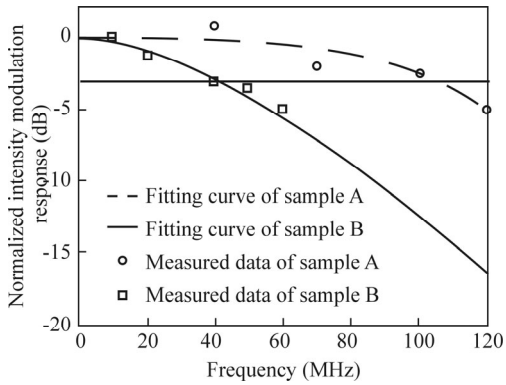

Fig.3 Intensity modulation responses of samples A and B at 50 mA bias current

We have investigated the steady and dynamic characteristics of the n-doped and non-doped InGaN LEDs by implementing their equivalent Spice model on a SPICE circuit. Simulation results show good agreement with Shi's measured experimental data. The improvement of LED's performance can be attributed to the enhanced ratiative rate due to the n-type doping in the barrier.

References

[1] J. Shakya, K. Knabe, K. H. Kim, J. Li, J. Y. Lin and H. X. Jiang, Appl. Phys. Lett. **86**, 091107 (2005).

[2] C. H. Wang, C. C. Ke, C. Y. Lee, S. P. Chang, W. T. Chang, J. C. Li, Z. Y. Li, H. C. Yang, H. C. Kuo, T. C. Lu and S. C. Wang, Appl. Phys. Lett. **97**, 261103 (2010).

[3] Zhiqiang Liu, Tongbo Wei, Enqing Guo, Xiaoyan Yi, Liancheng Wang, Junxi Wang, Guohong Wang, Yi Shi, Ian Ferguson and Jinmin Li, Appl. Phys. Lett. **99**, 091104 (2011).

[4] J. J. D. McKendry, R. P. Green, A. E. Kelly and Z. Gong, IEEE Photon. Technol. Lett. **22**, 1346 (2010).

[5] J. J. D. McKendry, D. Massoubre, S. Zhang, B. R. Rae and R. P. Green, J. Lightwave Technol. **30**, 61 (2012).

[6] J. W. Shi, H. Y. Huang and J. K. Sheu, IEEE Photon. Technol. Lett. **18**, 1636 (2006).

[7] J. W. Shi, P. Y. Chen and C. C. Chen, IEEE Photon. Technol. Lett. **20**, 1896 (2008).

[8] Han-Youl Ryu, Hyun-Sung Kim and Jong-In Shim, Appl. Phys. Lett. **95**, 081114 (2009).

[9] W. T. Tsang, Semiconductor Injected Lasers and Light Emitting Diodes, Beijing: Press of Tsinghua University, 1991.

[10] Sheng-Hormg, Miao-Chan Tsai, Meng-Lun Tsai, Yu-Jiun Shen, Ta-Cheng Hsu and Yen-Kuang Kuo, IEEE Photon. Technol. Lett. **21**, 975 (2009).

[11] Yen-Kuang Kuo, Miao-Chan Tsai, Sheng-Horng Yen, Ta-Cheng Hsu and Yu-Jiun Shen, IEEE Quantum Electron. **46**, 1214 (2010).